International Journal of Advance Research in Science and Engineering
Volume No. 12, Issue No. 07, July 2023
www.ijarse.com
IJARSE
ISSN 2319 - 8354

TRANSIENT GALACTIC COSMIC-RAY MODULATION DURING SOLAR CYCLE 24: A COMPARATIVE STUDY OF TWO PROMINENT FORBUSH DECREASE EVENTS

[1]Dharmendra Kumar Sharma, *Department of physics, APSU Rewa (M.P.)*

E-mail: dheeru.sharmaj111@gmail.com

[2]Dr Achyut Pandey, *Professor and Head, Department of Physics Govt., T.R.S. College Rewa*

E-mail: achyut.pandey9@gmail.com

[3]Kirti Mishra, *Department of Physics, APSU Rewa (M.P.)*

E-mail: km290991@gmail.com

ABSTRACT

Forbush decrease (FD) events are of great interest for transient galactic cosmic-ray (GCR) modulation study. In this study, we perform comparative analysis of two prominent Forbush events during cycle 24, occurring on 2012 March 8 (Event 1) and 2015 June 22 (Event 2), utilizing the measurements from the worldwide neutron monitor (NM) network. Despite their comparable magnitudes, the two Forbush events are distinctly different in terms of evolving GCR energy spectrum and energy dependence of the recovery time. The recovery time of Event 1 is strongly dependent on the median energy, compared to the nearly constant recovery time of Event 2 over the studied energy range. Additionally, while the evolutions of the energy spectra during the two FD events exhibit similar variation patterns, the spectrum of Event 2 is significantly harder, especially at the time of deepest depression. These difference are essentially related to their associated solar wind disturbances. Event 1 is associated with a complicated shock-associated interplanetary coronal mass ejection (ICME) disturbance with large radial extent, probably formed by the merging of multiple shocks and transient flows, and which delivered a glancing blow to Earth. Conversely, Event 2 is accompanied by a relatively simple halo ICME with small radial extent that hit Earth more head-on.

***Key words**: cosmic rays – Sun: activity – Sun: coronal mass ejections (CMEs)*

1. INTRODUCTION

Forbush decreases (FDs) are transient and rapid depressions in the galactic cosmic-ray (GCR) intensity, which are typically characterized by a sudden decrease reaching a minimum within about 1 day, sustained for a few hours to several days before the subsequent more gradual recovery phase lasting from several days up to a few weeks (Lockwood 1971; Cane 2000). While FDs were first observed by Forbush (1937) and Hess &

Demmelmair (1937) using ionization chambers on Earth, measurements from a wide variety of spacecraft have shown that they are also present on other planets (e.g., Martian surface) and in the interplanetary space distant from planets (e.g., Ahluwalia et al. 2009; Hassler et al. 2014). Therefore, the Forbush effect is universal within the heliosphere. The FDs are of great interest for both space weather application and the study of transient GCR modulation (Kuwabara et al. 2009). Specifically, a detailed analysis of FD events should shed light on physical processes that are most important for the propagation of energetic particles through the perturbed medium. Despite decades of progress, the worldwide network of ground-based neutron monitors (NMs), covering a wide range of geomagnetic latitudes and longitudes, remains the state-of-the-art instrumentation for measuring cosmic rays with energies up to tens of GeV. It was until very recently that the shape of the GCR spectrum during an FD was directly measured by the PAMELA (Payload for Antimatter Matter Exploration and Light-nuclei Astrophysics) instrument (Adriani et al. 2011; Usoskin et al. 2015). Long-term groundbased observations, as well as in situ solar and interplanetary observations, have greatly increased our understanding of the underlying physics of FDs. It is widely, although not universally, accepted that most FDs are caused by the passage of large-scale solar wind disturbance related to corotating interplanetary regions (CIRs) or Earth-directed coronal mass ejections (CMEs) from the Sun and their associated shocks (Cane 2000). CMEs are large, twisted magnetic structures that are expelled from the solar corona out into the heliosphere with speeds ranging from a few hundred up to 3000 km s−1 . If the speed of the CME exceeds that of the surrounding solar wind by greater than the fast magnetosonic wave speed, it will drive an interplanetary shock (IS) front (Richardson & Cane 2010). Such CMEs expand and propagate in interplanetary space, transforming into what are commonly called interplanetary CMEs (ICMEs). CME–CME interactions are relatively common phenomena during the solar maximum. Occasionally, fast ICMEs may interact with the preceding slow ICMEs, merging into a complicated compound interplanetary disturbance (Burlaga et al. 2001; Maričić et al. 2014). Yermolaev et al. (2015) summarized dynamic characteristics of the plasma and field parameters of eight sequences of solar wind disturbances, including CIR, IS/CIR, Ejecta, Sheath/Ejecta, IS/Sheath/Ejecta, MC (Magnetic Cloud), Sheath/MC, and IS/Sheath/MC, which are generally characterized by enhanced solar wind bulk speed and strengthened interplanetary magnetic field (IMF) and turbulence level. These large, fast Earth-directed structures can sweep away GCR particles, leading to reductions of GCR intensities in the form of FDs with different shapes, and thus have pronounced effects on transient cosmic-ray modulation both locally and remotely. Particularly, the shockassociated ICMEs provide a natural explanation for the classical two-step FDs (Barnden 1973; Ifedili 2004). The initial step of fast-decreasing intensity coincides with the passage of a magnetically turbulent high-field region (e.g., shock/sheath). Then, the next step of the intensity decrease is concurrent with the passage of a magnetically quiet high-field region (e.g., CME ejecta/magnetic cloud), and the recovery phase starts after the passage of this disturbance. In general, the shock/sheath and the ejecta/MC contributions to the overall

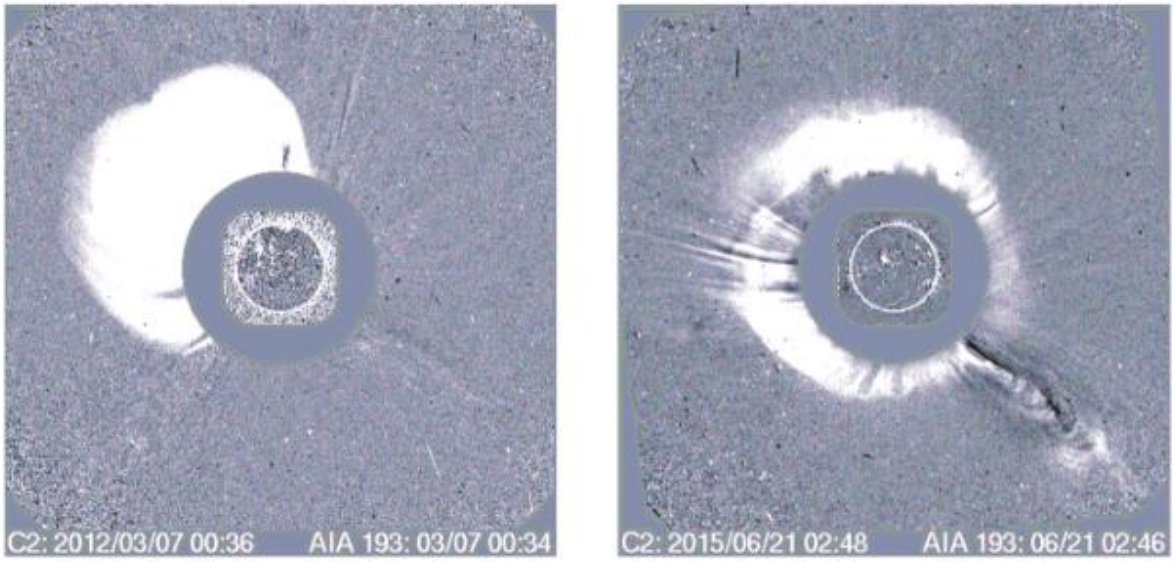

Figure 1. LASCO C2 images of the CMEs on 2012 March 7 at 00:36 UT (left) and 2015 June 21 at 02:48 UT (right).

magnitude of the decrease vary, and the time profiles of the decrease due to these two effects can be distinctly different. Although the cause and the general shape of FDs are relatively well understood, theoretical treatments of this phenomenon are still in their infancy and cannot completely explain the detailed shape of FDs. The current standard theory of the classical two-step FD model predicts an energydependent FD magnitude, which is directly proportional to the magnetic field strength and turbulence in the associated interplanetary disturbance (Belov et al. 2014). In contrast, the recovery time is expected to be energy independent and is only related to the transit speed of the ICME after it passes the observer. This classical model is, however, frequently violated in parctice (Ifedili 2004; Jordan et al. 2011). For instance, Penna & Quillen (2005) found that the fast ICMEs tend to cause stronger Forbush events with longer recovery times. Besides, whether the recovery time of FDs depends on the rigidity/energy remains a subject of intense controversy (e.g., Lockwood et al. 1986; Mulder & Moraal 1986). Usoskin et al. (2008) presented a thorough empirical study of the recovery phase of strong isolated FDs and showed that all the FDs with magnitude exceeding 10% demonstrate an energy dependence of the recovery time. GCR modulation during the recent unusual solar minimum between cycles 23 and 24 and the successive moderate solar maximum of cycle 24 have been investigated extensively (e.g., Alania et al. 2014). The observed modulation, which reached its maximum phase around 2013 (Ahluwalia & Ygbuhay 2015), is modest compared to previous cycles. Interestingly, while the sunspot number in this cycle has been 40% lower than that in cycle 23, more halo CMEs have been observed to occur at a higher rate during solar cycle 24 (Petrie 2015). Furthermore, the cycle 24 CMEs are significantly wider than their cycle 23 counterparts without being significantly faster. This anomalous CME expansion is generally attributed to the decrease of the heliospheric total pressure (Gopalswamy et al. 2014, 2015). As a consequence, CMEs have diluted magnetic energy content because of their greater expansion and interaction with weaker ambient heliospheric fields. Despite the enhanced rates of halo CMEs, the fast/large CMEs are rare for cycle 24, resulting in a smaller number of FDs during this period. The first significant FD of solar cycle 24 was recorded in 2011 February 18 (Oh & Yi 2012),

and it was not until 2012 May 17 that the first ground-level enhancement of solar cycle 24 occurred (Gopalswamy et al. 2013). Until now, there have been two prominent FDs with magnitude ∼10% during cycle 24, which occurred on 2012 March 08 and 2015 June 22, respectively. In this study, we comparatively analyze the characteristics of the two relatively strong FD events in detail, using the records from the worldwide NM network, together with the in situ measurements of the interplanetary plasma and field parameters during the passage of the corresponding ICMEs. The organization of the paper is as follows: Details of the two events are described in Section 2. Section 3 presents the statistical analysis, and further discussions are addressed in Section 4. The last section provides a summary and conclusions

2. TWO UNUSUAL FD EVENTS DURING CYCLE 24

As the solar activity was approaching its maximum during solar cycle 24, an X-ray flare (X5.4 class) occurred in NOAA AR 11429 at 00:02 UT on 2012 March 7 (flare onset time), associated with an intense halo CME with a peak speed of about 2684 km s−1 , and followed by a smaller flare (X1.3 class) about 1.5 hr later. After that, a series of M-class flares and large CMEs occurred within the same region, including an M6.3 flare around 03:30 UT on March 9, an M8.4 flare around 17:30 UT on March 10, and an M7.9 flare around 17:30 UT on March 13. On 2015 June 21 (01:02 UT), an M2.0-class solar flare located at N12°E13°, in conjunction with another halo CME, was observed.

Figure 1 shows the C2 coronagraph observations of the two CMEs by the SOlar and Heliospheric Observatory (SOHO; Domingo et al. 1995) Large Angle and Spectrometric Coronagraph Experiment (LASCO; Brueckner et al. 1995). Both CMEs caused strong Forbush events that were obviously recorded by the worldwide network of NMs approximately 35 hr and 41 hr after their occurrence, respectively. Besides, their recovery phase is remarkably clear, without being significantly distorted by the other transient events.

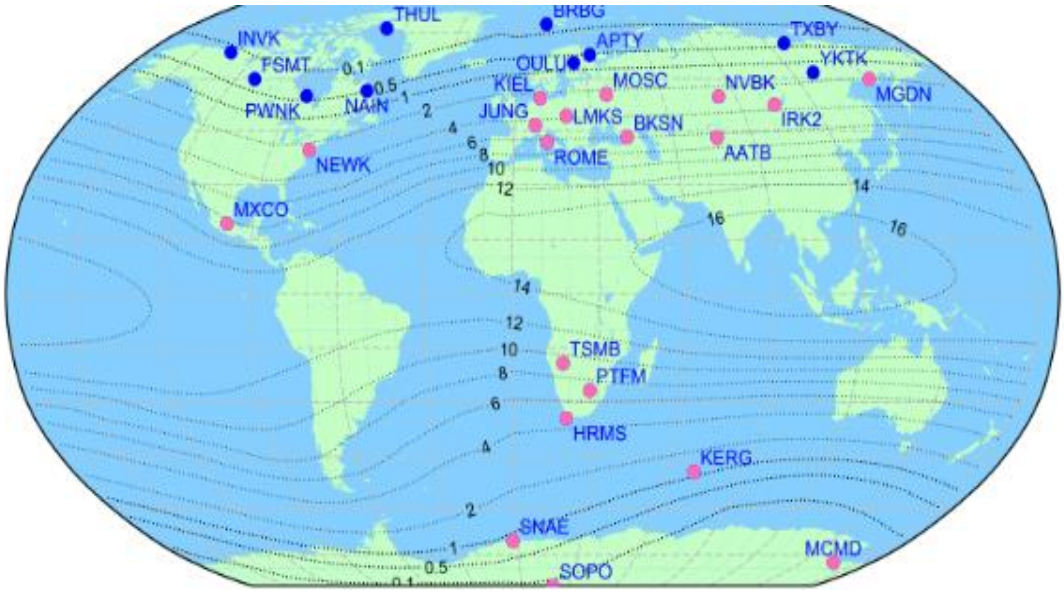

Figure 2. Distribution of NM stations used in this analysis, along with a world map of vertical cutoff rigidity contours for Epoch 2000 from Smart & Shea (2008). Note that the contours are in units of rigidity (GV).

IJARSE
ISSN 2319 - 8354

Hereafter, we refer to the two FD events on 2015 March 8 and 2015 June 22 as Event 1 and Event 2, respectively. We use the measurements from the worldwide NM network to pinpoint the characteristics of the recorded FDs. Figure 2 shows the distribution of the NM stations used in this study, along with the vertical cutoff rigidities from Smart & Shea (2008). Detailed information about these NM stations is also listed in Table 1

from NM stations with the in situ measurements of several interplanetary plasma/field parameters from the Advanced Composition Explorer (ACE) spacecraft located at Lagrange point L1 (Stone et al. 1998). It should be noted that all the count rates are set relative to the average value over several undisturbed days preceding the events, to emphasize relative changes in the GCR fluxes and minimize the uncertainties ascribed to diurnal variations in the count rates. Figures 3 and 4 show the hourly averaged time profiles of the vector IMF magnitude |B|, the standard deviation of IMF vector dB, and the solar wind velocity Vsw from the ACE spacecraft during the periods of Event 1 and Event 2, respectively. Moreover, the relative changes of the pressure-corrected hourly count rate of the SOPO NM station (Rc = 0.1 GV) are also shown for comparison. The gray shaded regions mark the main phases of the two FD events, which cover the period from the onset of the sharp decrease to the beginning of the recover phase, and a zoom-in of these is shown in the right panels for the purpose of clear presentation.

We note that the time shift (calculated according to the spacecraft observations and reasonable estimates) between the ACE spacecraft and Earth has been taken into account for plotting Figures 3 and 4. Event 1 appears to be a classical two-step FD associated with a fast compound solar wind structure. The fast CME of 2012 March 7 has been investigated in detail by various previous studies (e.g., Davies et al. 2013; Liu et al. 2013; Rollett et al. 2014).

This event is of particular interest partly due to the fact that it occurred within a series of other CMEs. Therefore, CME–CME interactions are likely, and evidence for this is seen in the wide-angle heliospheric imaging observations (Liu et al. 2013). Besides, multipoint observations in interplanetary space suggest that the CME propagates east of the Sun–Earth line (Rollett et al. 2014), implying that it probably delivers a glancing blow to Earth. The arrival of the IS wave at Earth, which is marked by the dashed line in Figure 3, was identified by the sudden increase of the IMF magnitude and the solar wind bulk speed at 10:19 UT on 2012 March 08 (Liu et al. 2013), concurrent with the onset time of Event 1. Meanwhile, the count rate decreases sharply and reaches the depth of ~15% within several hours, and subsequently remains depressed for about 1 day before the initial gradual recovery. Note that this recovery process is interrupted by the arrival of another disturbance 4 days later (2012 March 12).

Rollett et al. (2014) show that preceding large CME events may disturb the overall shape of the ensuing CME and influence its propagation behavior. Therefore, the two disturbances on 2012 March 8 and 12 may merge into a compound ICME structure, which include multiple shock and transient flows, leading to large radial extent and possible latitudinal and longitudinal departure. The GCR count rate gradually returns to the pre-decrease

IJARSE
ISSN 2319 - 8354

level, about 11 days after the passage of this compound solar wind disturbance over Earth. In contrast to the complex GCR variation structure of Event 1, the time profile of Event 2 appears to be simpler. We observe that the GCR count rate decrease started on 2015 June 22 at 19:00 UT and reached the maximum depression (~10%) wthin about 3 hr, followed by a sustained depression for

Table 1

List of the Neutron Monitor Stations Used in This Study

No.	NM Station	Abbrev.	Longitude (deg)	Latitude (deg)	Altitude (m)	R_c (GV)	E_m (GeV)
1	Almaty	AATB	76.60	43.14	3340	6.69	15.08
2	Apatity	APTY	33.40	67.57	181	0.65	10.23
3	Baksan	BKSN	42.69	43.28	1700	5.60	13.73
4	Barentsburg	BRBG	14.42	78.12	L	0.20	10.15
5	Fort Smith	FSMT	−111.93	60.02	180	0.30	10.17
6	Hermanus	HRMS	19.22	−34.42	26	4.90	12.98
7	Inuvik	INVK	−133.72	68.36	21	0.30	10.17
8	Irkutsk	IRK2	104.03	52.47	2000	3.64	11.84
9	Jungfraujoch	JUNG	7.98	46.55	3570	4.50	12.57
10	Kerguelen	KERG	70.25	−49.35	33	1.14	10.41
11	Kiel	KIEL	10.12	54.34	54	2.36	10.97
12	Lomnicky Stit	LMKS	20.22	49.20	2634	3.84	12.00
13	McMurdo	MCMD	166.72	−77.85	48	0.01	10.12
14	Magadan	MGDN	151.05	60.04	220	2.09	10.82
15	Moscow	MOSC	37.32	55.47	200	2.43	11.01
16	Mexico City	MXCO	−99.18	19.33	2274	9.53	19.55
17	Nain	NAIN	−61.68	56.55	46	0.30	10.17
18	Novosibirsk	NVBK	83.00	54.80	163	2.91	11.31
19	Newark	NEWK	−75.75	39.68	50	2.40	10.99
20	Oulu	OULU	25.47	65.05	15	0.81	10.30
21	Potchefstroom	PTFM	27.10	−26.68	1351	7.30	15.92
22	Peawanuck	PWNK	−85.44	54.98	53	0.30	10.17
23	Rome	ROME	12.47	41.86	0	6.27	14.53
24	Sanae	SNAE	−2.35	−70.30	52	1.06	10.38
25	South Pole	SOPO	0.00	−90.00	2820	0.10	10.14
26	Thule	THUL	−68.70	76.50	26	0.30	10.17
27	Tsumeb	TSMB	17.58	−19.20	1240	9.29	19.12
28	Tixie Bay	TXBY	128.54	71.36	0	0.48	10.21
29	Yakutsk	YKTK	129.43	62.01	105	1.65	10.61

about 2 days, and then a recovery to pre-decrease level taking a much longer time. Concurrently, there is a dramatic increase in the solar wind velocity, as well as a brief and small spike in both the magnetic field magnitude B| and its variance dB. While the solar wind velocity remains enhanced for a longer period, the IMF magnitude decreases quickly to the back- ground level.

Although the kinematics and the shape of the ejection cannot be strictly constrained due to lack of wide-angle heliospheric imaging observations, the relatively simple time profile of the interplanetary parameters, as well as the GCR intensity, suggests that Event 2 corresponds to the passage of a relatively simple modulating structure in near-Earth space, probably a single shock-associated CME ejecta structure. Moreover, the halo CME on 2015 June 21 appears to be more symmetric

(Figure 1), suggesting that it probably hit Earth more head-on than the CME on 2012 March 7.

3. DATA ANALYSIS

Following the usual method (e.g., Lockwood et al. 1991; Usoskin et al. 2008), the characteristic energy of each NM station (i.e., the median energy E_M) is defined so that cosmic rays with energy (or below) E_M contribute half

to the detector's count rate. The median energy E_M of an NM can be approximately related to its cutoff rigidity P_c with Equation (1) (Jämsén et al. 2007; Usoskin et al. 2008):

$$E_m = 0.0877P^2 + 0.154P_c + 10.12$$

where E_M and P_c are expressed in GeV and GV, respectively. The median energies range from ∼10 GeV for the polar NM stations to ∼20 GeV for the equatorial NM stations, which enable us to investigate the energy dependence (or indepen- dence) characteristics of the two FD events. While the muon telescope data can help to extend the knowledge about FDs to energies beyond the NM regime, unfortunately no muon telescope data are publicly available during the studied period.

3.1. Precursory Increase

Figure 5(a) presents relative count rate changes of several selected NM stations (MXCO, ROME, HRMS, JUNG, MOSC, OULU, THUL, SOPO) for Event 1. It is noted that these time profiles are vertically shifted for the purpose of presentation.

One interesting feature of Event 1 is the pre-increase structure that is clearly observed by most NMs, which are denoted as pink filled circles in Figure 2, except a few high-latitude ones located at the northern hemisphere with cutoff rigidity lower than 2 GV. There is a slight spread in the peak timing of the pre-increase due to the stations of different longitudes essentially providing different viewing angles into the helio- sphere. This precursory increase is a typical feature of FDs due to shock-associated ICMEs and is commonly attributed to reflection of particles from the shock or shock acceleration (Papailiou et al. 2012). However, the fact that it

is absent only from the observations of the NM stations at the high-latitude northern hemisphere is surprising. Figure 6 shows scatter plots of the pre-increase magnitude versus the medium energy of NM stations are about a few percent magnitude, which are comparable to pre-increase magnitudes. Hence, we only showthe results of a few NM stations with weak diurnal variations,

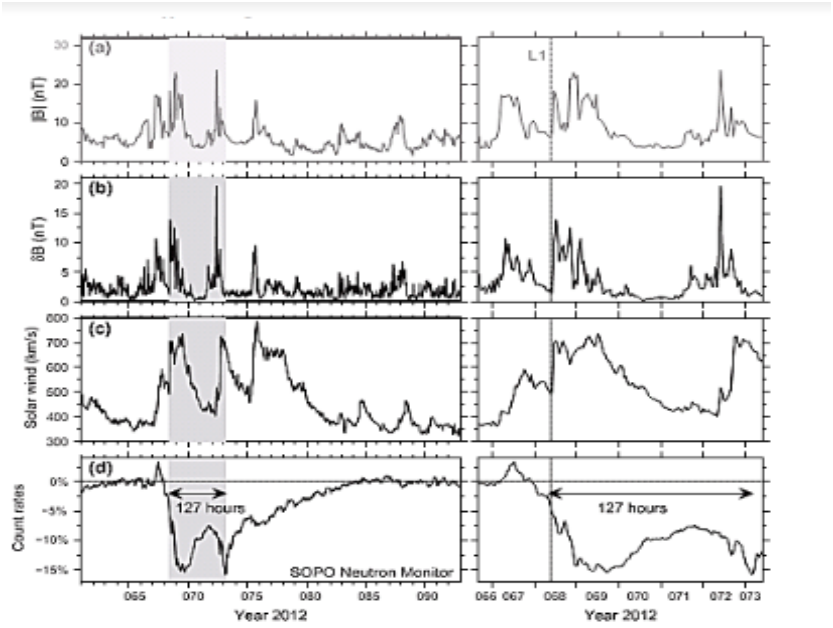

Figure 3. *ACE* and SOPO NM observations during the first Forbush event (Event 1) from 2012 March 1 at 00:00 UT to 2012 April 1 at 23:00 UT. (a) IMF magnitude $B|$; (b) standard deviation of IMF vector dB; (c) solar wind speed V_{sw}; (d) relative changes of pressure-corrected hourly count rates of SOPO NM station. The dashed line (L1) indicates the IP shock arrival time.

And thus the pre-event and pre-increase can be clearly and unambiguously defined. Although scattered, we do see a weakly energy-dependent pre-increase magnitude (Figure 6).

3.1. Evolving GCR Energy Spectrum

The magnitude of FD events is generally energy/rigidity dependent, well described by a power law (Cane 2000). Here we study the energy dependence of the amplitudes of the two large FDs that occurred during the solar cycle 24.

Similar to Figure 5, Figure 7(a) also presents relative count rate changes of several selected NM stations (MXCO, ROME,BKSN, JUNG, MOSC, OULU, THUL, SOPO) for Event 2.

We define the amplitude of the two FDs as the averaged value of the relative counting rate over the short time interval (~24 hr) just after the sharp decrease (gray shaded regions in Figures 5(a) and 7(a)). Figure 5(c) shows the amplitudes of Event 1 as a function of median energy over the energy range from 10 to 20 GeV, and Figure 7(c) presents the similar resultsof Event 2. We performed a linear regression analysis of the

depression magnitude with the median energy. In both cases, the amplitudes are found to be a power law, with negative exponents $\gamma = 1.23 \pm 0.08$ ($R = -0.95$) and $\gamma = 1.11 \pm 0.12$

(R = −0.89), respectively. Our results are generally consistent with previous studies (e.g., Ahluwalia et al. 2009, 2014; Ahluwalia & Ygbuhay 2015).

We also investigate the evolution of the energy-dependent modulation through the major and subsequent recovery phasesof the FD events. In order to remove the diurnal variation and obtain a statistically reliable value of amplitudes, we apply a running 24 hr average to the hourly relative count rate data over the studied period.

Figure 8(a) (top) presents the smoothed relative count rates of Event 1 for the NM stations MXCO (black), HRMS (blue), and MOSC (red). Assuming power-law energy dependence of the GCR intensity variation, we obtain the temporal variation of the exponent γ, which is shown in Figure 8(a) (bottom). Figure 8(b) presents similar results for Event 2. As expected, the exponent γ of the two FD events exhibits a similar variation pattern. At the initial phase, the energy spectrum is relatively soft, and it gradually becomes harder up to the time of the minimum level of the GCR intensity. Subsequently, the energy spectrum gradually becomes softer during the recovery phase. Note the excursion due to the arrival of the later modulating structure around 2012March 14. Nevertheless, the energy spectrum of Event 2 is remarkably harder than that of Event 1, especially at the time ofdeepest depression.

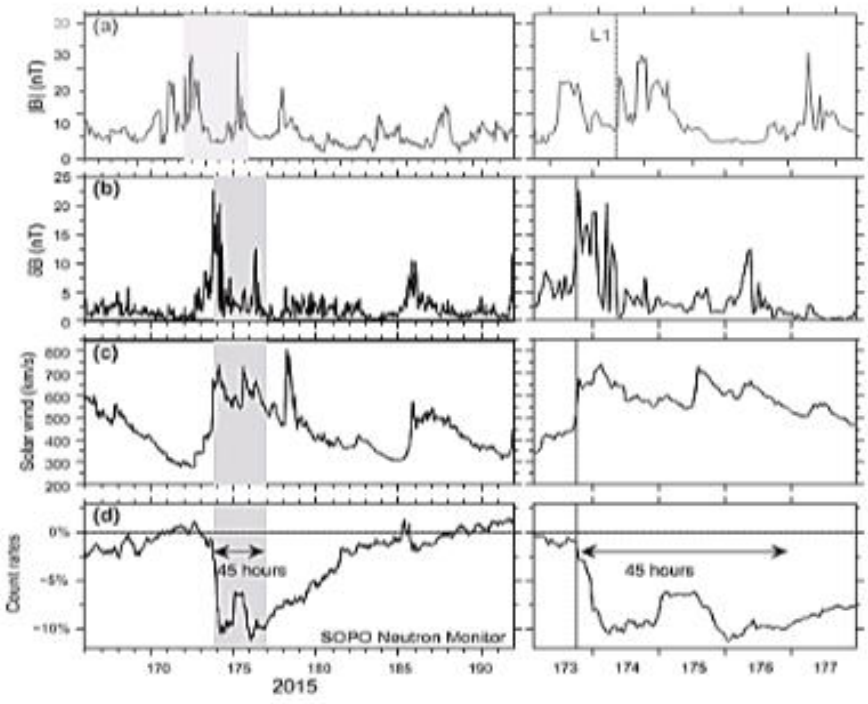

Fig.4. Same as Figure 3, but for the second Forbush event (Event 2) from 2015 June 15 at 00:00 UT to 2015 July 10 at 23:00 UT. The dashed lines (L1) indicatesthe IP shock arrival time.

3.1. Recovery Time

We also used the NM count rates to investigate the gradual recovery of the two Forbush events. From Figures 5 and 7, wecan see that the recovery phase of the two FD events took about10 days, with clearly diurnal variations of a few percent magnitude. In addition, its shape is close to an exponential in time and is characterized by the

recovery time τ. Thus, the recovery time has been defined by fitting the observed time profile of the relative intensity (blue lines in Figures 5(a) and 7(a)) with the exponentials of the form given by Equation (2), individually for each detector but for the same time interval

$$\delta I = \frac{I_0 - I}{I_0} = A \cdot \exp\left(-\frac{t - t_0}{\tau}\right) \qquad (2)$$

Where I_0 is the pre-event level, A the depression magnitude, and t_0 the time when the recovery starts. The best-fit exponentials tothe recovery phases of the Forbush events are also shown (solid red lines in Figures 5(a) and 7(a)). Recovery time measurement errors are mainly caused by noise in the count rates and their fluctuations associated with later solar wind disturbances. In order to check the stability of the results, we test different starting time t_0 and ending time, and we find that the recovery time generally varies within 5 hr.

The recovery time τ is plotted versus the median energy of detectors for Event 1 (Figure 5(b)) and Event 2 (Figure 7(b)). Itis evident that the recovery time of Event 1 strongly depends on the median energy, which decreases from 125 hr for the polarNM stations to 88 hr for the two near-equatorial NM stations (MXCO and TSMB). Conversely, the recovery time of Event 2, although somewhat scattered, remains almost constant (~95 hr) over the studied energy range.

4. DISCUSSIONS

In this work, we mainly focus on the characteristics of the two studied FDs recorded by the worldwide NM network, rather than the global shape and propagation of CMEs in the whole Sun–Earth space, which could be extremely complicated due to the possible interaction and intermingling between successive CMEs (Liu et al. 2013, 2016). Although both the studied FDs are most probably triggered by ICMEs, they are quite different in terms of evolving GCR energy spectrum and energy dependence of the recovery time. While both the magnetic field magnitude and its variance during Event 1 are significantly lower than those of Event 2, the magnitude of Event 1 is obviously larger. Besides the strength of the magnetic fields in the ICME, several other factors, such as the size of the ICME and the proximity of the

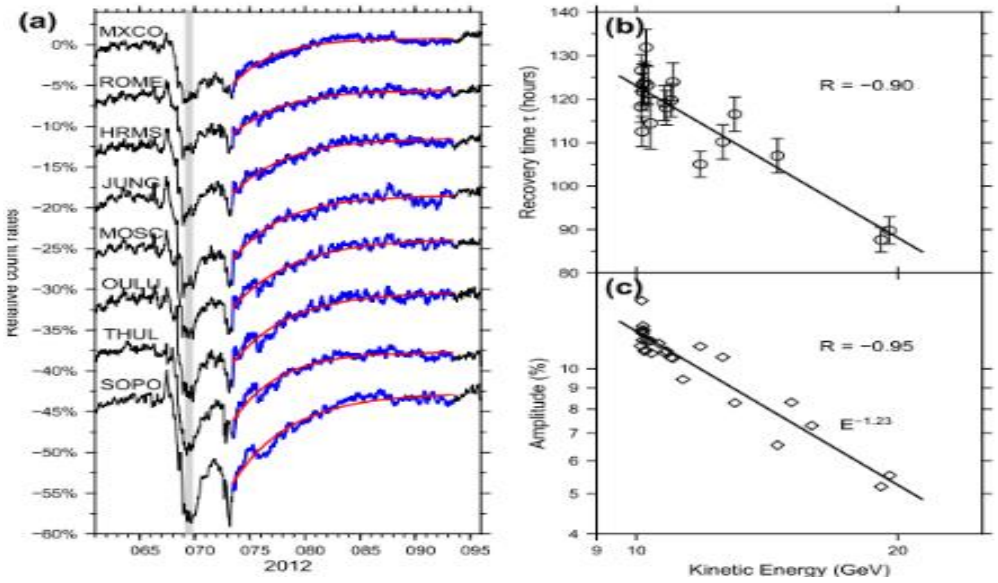

Figure 5. (a) Relative count rate changes of Event 1 for several selected NM stations. Note that the time profiles are vertically shifted for the purpose of presentation. The blue lines represent the data used for fitting, and the red lines indicate the best-fit exponential to the recovery phase. (b) Recovery time τ of Event 1 as a function of median energy. (c) Amplitudes of Event 1 as a function of median energy

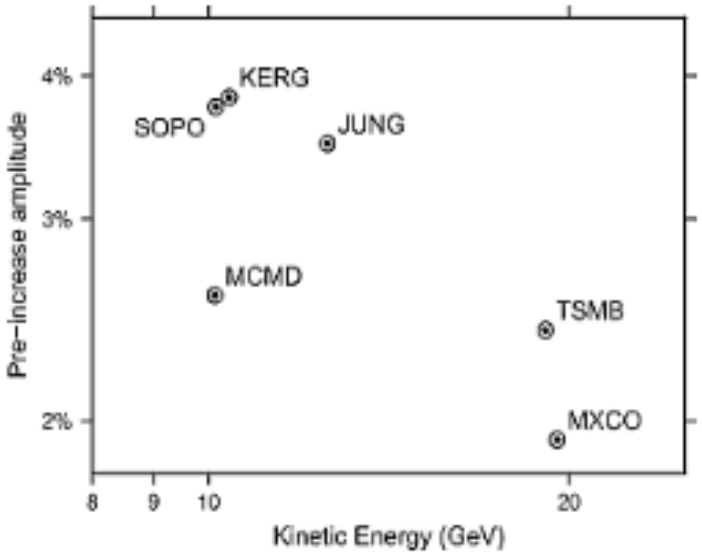

Figure 6. Pre-increase magnitude of several NM stations as a function of the medium energy for Event 1.

CME to the Earth, can also contribute to the magnitude of FD events (Patra et al. 2011). In our case, we attribute the large magnitude of Event 1 to the large radial extent of the complicated shock-associated ICME. Based on the durations (~127 and ~45 hr) and the average solar wind speed (~600 km s−1), the radial extent of the two ejecta is estimated to be ~1.8 au and ~0.6 au, respectively. From the measurements of interplanetary

plasma/field parameters presented in Figure 3, we can see that Event 1 is associated with a compound solar wind disturbance, probably formed due to interaction of a series of successive halo CMEs of various sizes, including the disturbance on 2012 March 12. Since Event 2 is related to a single transient flow, the strong IMF and its variance during Event 2 are possibly responsible for the large FD magnitude, emphasizing the importance of the turbulent field region in depressing the GCR intensity. A dependence of the amplitude on the rigidity/energy of GCR particles is one of the fundamental characteristics of FDs (Alania & Wawrzynczak 2008). FDs are essentially due to the effect of relatively strong, ordered magnetic fields on the turbulent diffusion of cosmic rays (Cane 2000). The plasma inside the CME is of coronal origin and is largely devoid of high-energy cosmic rays. As the shock passes Earth, it acts as a shield of sorts against the ambient population of cosmic rays, since they cannot easily diffuse across the enhanced magnetic field in the vicinity of the shock. Consequently, the interior of the CME has a lower density of cosmic rays in comparison to its surroundings. Similarly, the diffusion of the ambient cosmic rays into the CME ejecta/MC is further inhibited due to the relatively organized, large-scale magnetic field that encloses it. Be smaller for cosmic rays at higher energies (Alania & Wawrzynczak 2012). Moreover, stronger magnetic field strength and turbulence level should produce a harder GCR energy spectrum (Adriani et al. 2011). Thus, the energy spectrum exponent ($\gamma = 1.11$) of Event 2 is slightly smaller than that of Event 1 ($\gamma = 1.23$).

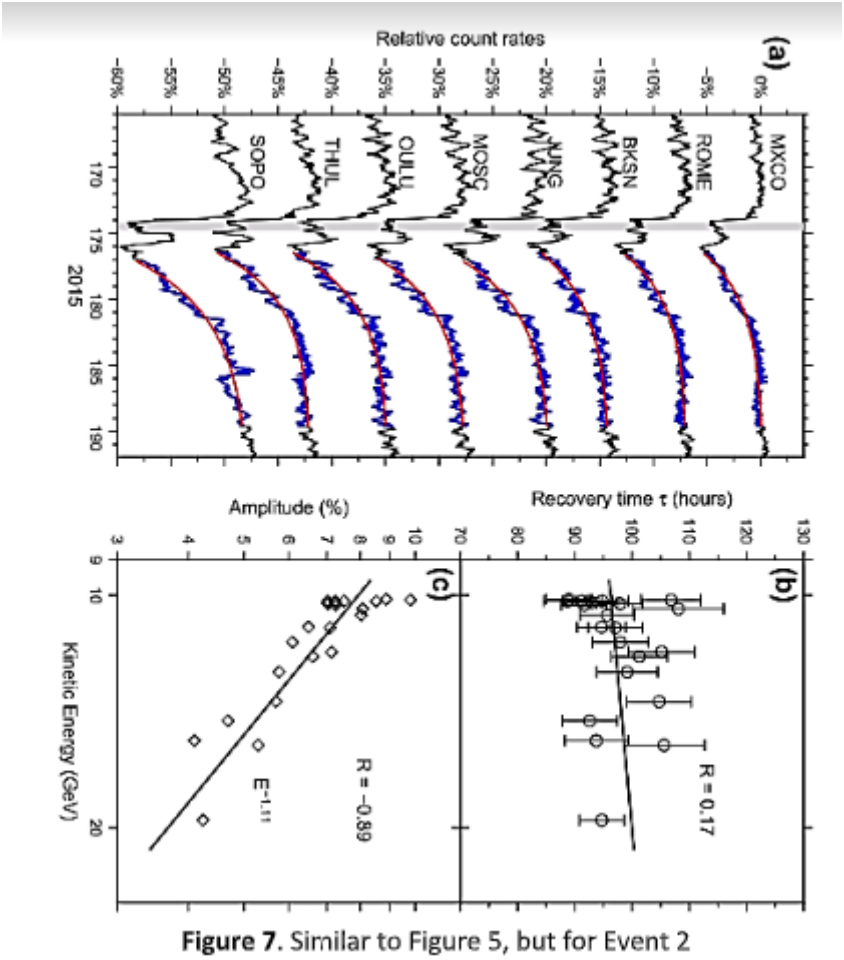

Figure 7. Similar to Figure 5, but for Event 2

IJARSE
ISSN 2319 - 8354

Additionally, the temporal variation of the energy spectrum exponent is also closely related to the diffusion process, i.e., the state of the turbulence of the IMF (Wawrzynczak & Alania 2010; Alania et al. 2013). In both cases, the GCR spectra during the deep phase of the Forbush events appear much harder than during the quiet time, in agreement with the in situ GCR spectra measurements from the PAMELA experiment during a large FD event (Usoskin et al. 2015). It should be noted that the strong geomagnetic disturbance during major FDs may lead to slightly changed cutoff rigidities. Nevertheless, previous studies have shown that the temporary changes in the cutoff rigidity have negligible effects on the general features of the temporal changes in the rigidity spectrum of FDs (Alania & Wawrzynczak 2012; Alania et al. 2013)

The recovery time is another important characteristic parameter of Forbush events. In this study, the recovery time of Event 1 is notably longer than Event 2 and strongly depends on the kinematic energy, which contradict the standard theory. Generally, the recovery phase of an FD is mainly influenced by the dissipation effect of the shock modulation process. The radial departure of the shock and the longitudinal departure can both affect the recovery time (Penna & Quillen 2005).

The effect of the shock on GCR modulation near 1 au decreases with increasing radial distance of the shock moving farther away from Earth, which causes the gradual recovery process of the cosmic-ray intensity (e.g., le Roux & Potgieter 1991).

Such models imply that the recovery time of a Forbush event is independent of the depth of the decrease and the strength of its magnetic field, leading to little or no energy dependency of the recovery time. Yet, the recovery time is predicted to be shorter associated with the interplanetary disturbance with smaller radial extent. Since the transient usually has a limited longitudinal extent, the relative Sun–Earth geometry, in addition to the radial departure, may also play a critical role in damping of the shock modulation effect. Moreover, since the shocks have a greater longitudinal extent than ejecta, it is possible to intercept the shock but not the ejecta. When approaching the edge of the longitudinal range of the shock, higher-energy cosmic rays with larger gyroradii should recover more quickly, thereby causing the energy dependence of the recovery rate (Jämsén et al. 2007; Usoskin et al. 2008). The characteristic time of the recovery phase in this scenario is primarily determined by the longitudinal range of the shock, as well as the Earth's location relative to the shock during the main process of the FD (Usoskin et al. 2008). It should be pointed out that a number of

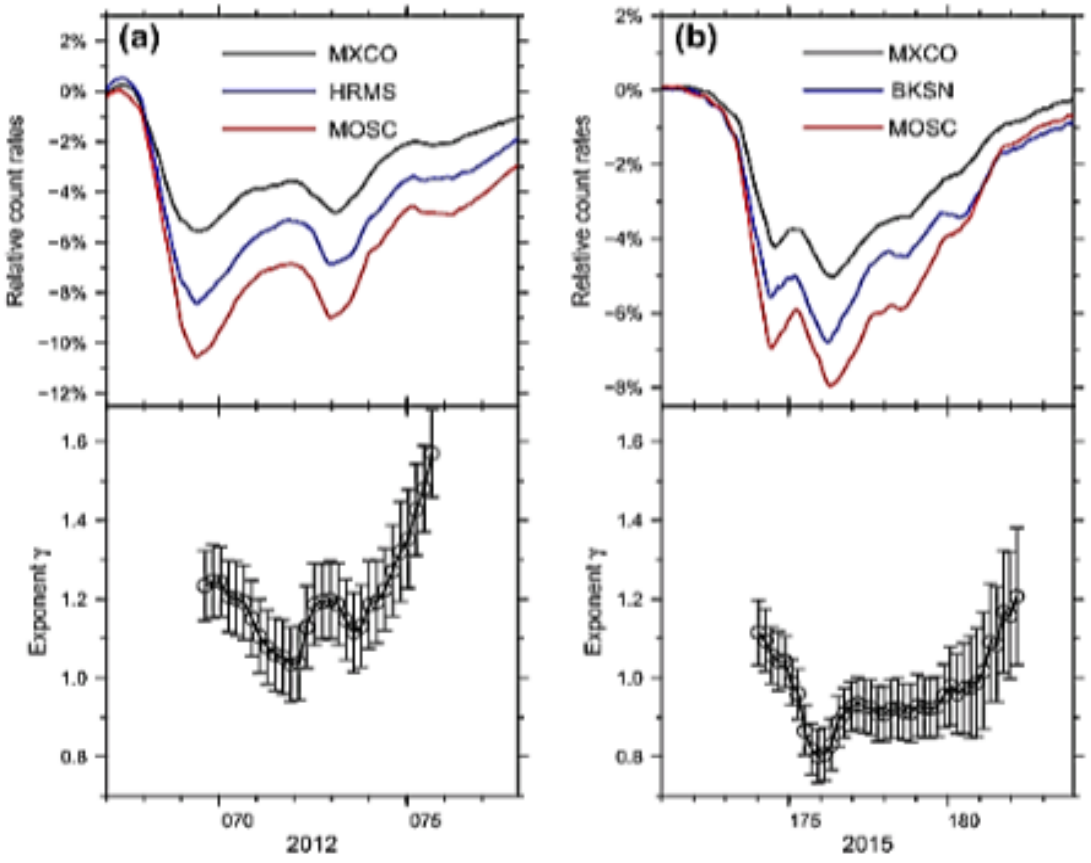

Figure 8. (a) Hourly relative count rates after applying 24 hr average (top) and the temporal variations of the energy spectrum exponent γ (bottom) for Event 1. (b) Similar to (a), but for Event 2.

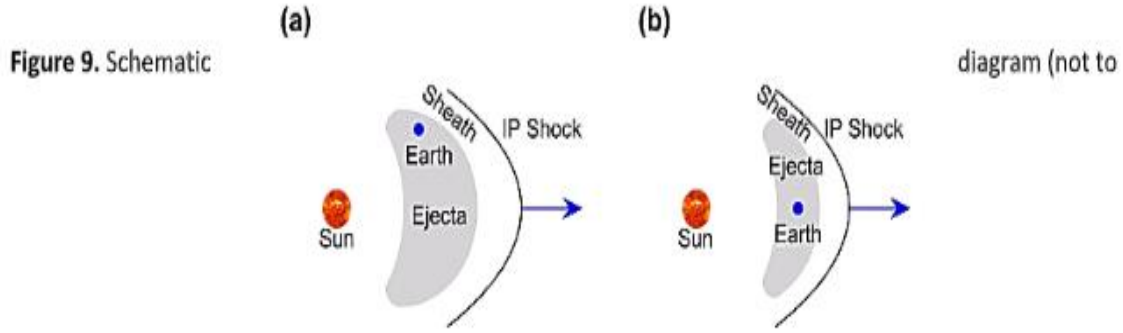

Figure 9. Schematic diagram (not to scale) explaining (a) Event 1 and (b) Event 2.

other factors could also affect the recovery time of a Forbush event, such as the gradient of the radial component of the cosmic-ray diffusion coefficient, the velocity of the ICME as it crosses Earth's orbit, and the deceleration rate of the ICME after it crosses Earth's orbit (Usoskin et al. 2008). Furthermore, ICMEs evolve in both size and

shape as they propagate outward, and the 3D parameters of ICMEs, especially the angular width, cannot be well constrained by a single view such as the LASCO on board SOHO (Lee et al. 2015). Based on the aforementioned discussions, we propose a simple schematic diagram explaining the formation of the two studied FD events (Figure 9). A CME, occurring at the Sun, propagates eastward and subsequently crosses Earth. The magnetic barrier, consisting of IP shock, Sheath, and Ejecta/ MC, acts as a strong shield against the energetic GCR particles. The different shapes of FDs are essentially related to their associated solar wind disturbances. It is conjectured that Event 1 might be associated with a complicated ICME structure, formed by the merging of multiple shocks and transient flows, leading to relatively large radial extent and possibly wide latitudinal and longitudinal width. However, the ICME propagates east of the Sun–Earth line, implying that it probably delivers a glancing blow to Earth.

The more glancing hit of the disturbance during Event 1 suggests a narrower longitudinal extent toward the west, resulting in energy dependence of the recovery time. In addition, the large radial extent is also responsible for the large depression magnitude of Event 1. On the contrary, Event 2 is accompanied by a relatively simple interplanetary disturbance of small radial extent, which possibly evolved from an overexpanded CME due to the declined heliospheric total pressure (Gopalswamy et al. 2015)

and hit Earth more head-on. Consequently, the radial departure determines the recovery time, which shows negligible energy dependence. Besides, the enhanced magnetic field strength and turbulence level also lead to a harder energy spectrum during the whole period of Event 2. In the future, more detailed modeling of the propagation of interplanetary transients and their dynamic effects on cosmicray transport is required to test the qualitative models and interpret the observational results presented in this study in a more quantitative way (e.g., Alania & Wawrzynczak 2008; Usoskin et al. 2015).

5. SUMMARY AND CONCLUSIONS

We comparatively analyze the characteristics of two intense Forbush events during solar cycle 24, using the continuous measurements from the worldwide NM stations. The two Forbush events are distinctly different in terms of the evolving GCR energy spectrum and the energy dependence of the recovery time. The recovery time of Event 1 is strongly dependent on the median energy, varying from 125 hr for the polar NM stations to 88 hr for the near-equatorial NM stations.

Conversely, the recovery time of Event 2 remains almost constant (~95 hr) over the studied energy range. The evolutions of the energy spectra during the two Forbush events exhibit similar variation patterns. The spectra are relatively soft at the initial phase, gradually getting harder up to the time of the minimum level of the GCR intensity, and progressively becoming softer again during the recovery phase. Nevertheless, the energy spectrum of Event 2 is remarkably harder than that of Event 1, especially at the time of the deepest depression. Those differences are essentially related to their associated solar wind disturbances. We conjecture that Event 1 is associated with a complicated shock-associated ICME with large radial extent, probably formed by the merging of multiple shocks and transient flows and which delivered a glancing blow to Earth. On the contrary, Event 2 is accompanied by a relatively simple halo ICME with small radial extent that hit Earth more head-on. The

comparison is interesting because it provides similarities and differences in the GCR intensity related to different solar wind structures. In this study, we only present two case studies that occurred during solar cycle 24. In the future, a comprehensive statistical investigation of the energy spectra evolution and the recovery times of more Forbush events, associated with various types of solar wind disturbances, might further help to clarity the occurrence mechanisms of different kinds of Forbush events. The observed different characteristics of Forbush events could be used to distinguish the structures and mechanisms responsible for transient cosmic-ray modulation. Such comparison will lead to further understanding of the underlying physics of energetic particle transport through the interplanetary medium and provide valuable insight into the transient GCR modulation. We are grateful to the constructive comments from the anonymous referee that significantly improved the manuscript. We acknowledge our colleagues who work hard to ensure stable operation of NM detectors at worldwide locations. We thank the ACE MAG, SWEPAM, and SIS instrument teams and the ACE Science Center for providing the ACE data (www. srl.caltech.edu/ACE/). This research work was supported by the National Science Foundation of China (41504133), the China Postdoctoral Science Foundation (2015M571097), the Science and Technology Development Fund of Macas SAR (FDCT) through grant 039/2013/A2, and the Special Program for Applied Research on Super Computation of the NSFCGuangdong Joint Fund (the second phase).

REFERENCES

1 . Adriani, O., Barbarino, G. C., Bazilevskaya, G. A., et al. 2011, ApJ, 742, 102Ahluwalia, H., Alania, M.,
2. Ahluwalia, H., & Ygbuhay, R. 2015, SoPh, 290, 635
3. Ahluwalia, H., Ygbuhay, R., & Duldig, M. 2009, AdSpR, 44, 58 Akiyama, S., et al. 2015, ApJL, 804, L23
4. Alania, M. V., & Wawrzynczak, A. 2012, AdSpR, 50, 725Barnden, L. R. 1973, Proc. ICRC (Denver), 1, 277
5. Alania, M. V., Modzelewska, R., & Wawrzynczak, A. 2014, JGR, 119, 4164 Alania, M. V., & Wawrzynczak, A. 2008, ASTRA, 4, 59
6. Alania, M., Wawrzynczak, A., Sdobnov, V., & Kravtsova, M. 2013, SoPh,286, 561
7. Belov, A., Abunin, A., Abunina, M., et al. 2014, SoPh, 289, 3949
8. Brueckner, G., Howard, R. A., Koomen, M. J., et al. 1995, SoPh, 162, 357Burlaga, L. F., Skoug,
9. R. M., Smith, C. W., et al. 2001, JGR, 106, 20957 Cane, H. V. 2000, SSRv, 93, 55
10. Davies, J. A., Perry, C. H., Trines, R. M. G. M., et al. 2013, ApJ, 777, 167 Domingo, V., Fleck, B., & Poland, A. 1995, SoPh, 162, 1 Forbush, S. E. 1937, PhRv, 51, 1108
11. Gopalswamy, N., Akiyama, S., Yashiro, S., et al. 2014, GeoRL, 41, 2673
12. Gopalswamy, N., Xie, H., Akiyama, S., et al. 2013, ApJL, 765, L30 Gopalswamy, N., Xie, H.,
13. Hassler, D. M., Zeitlin, C., Wimmer-Schweingruber, R. F., et al. 2014, Sci,343, 386
14. Hess, V. F., & Demmelmair, A. 1937, Natur, 140, 316Ifedili, S. O. 2004, JGR, 109, A02117
15. Jämsén, T., Usoskin, I. G., Räihä, T., Sarkamo, J., & Kovaltsov, G. A. 2007,AdSpR, 40, 342
16. Jordan, A. P., Spence, H. E., Blake, J. B., & Shaul, D. N. A. 2011, JGR, 116,A11103

17. Kuwabara, T., Bieber, J. W., Evenson, P., et al. 2009, JGR, 114, A05109le Roux, J. A., & Potgieter, M. S. 1991, A&A, 243, 531
18. Lee, H., Moon, Y.-J., Na, H., Jang, S., & Lee, J.-O. 2015, JGR, 120, 10237Liu, Y. D., Hu, H., Wang, C., et al. 2016, ApJS, 222, 23
19. Liu, Y. D., Luhmann, J. G., Lugaz, N., et al. 2013, ApJ, 769, 45Lockwood, J. A. 1971, SSRv, 12, 658 Lockwood, J. A., Webber, W. R., & Debrunner, H. 1991, JGR, 96, 5447Lockwood, J. A., Webber, W. R., & Jokipii, J. R. 1986, JGR, 91, 2851
20. Maričić, D., Vršnak, B., Dumbović, M., et al. 2014, SoPh, 289, 351 Mulder, M. S., & Moraal, H. 1986, ApJL, 303, L75 Oh, S. Y., & Yi, Y. 2012, SoPh, 280, 197
21. Papailiou, M., Mavromichalaki, H., Belov, A., Eroshenko, E., & Yanke, V.2012, SoPh, 276, 337
22. Patra, S. N., Ghosh, K., & Panja, S. 2011, Ap&SS, 334, 317Penna, R. F., & Quillen, A. C. 2005, JGR, 110, A09S05 Petrie, G. J. D. 2015, ApJ, 812, 74
23. Richardson, I., & Cane, H. 2010, SoPh, 264, 189
24. Rollett, T., Mostl, C., Temmer, M., et al. 2014, ApJL, 790, L6 Smart, D. F., & Shea, M. A. 2008, Proc. ICRC (Merida), 1, 737
25. Stone, E. C., Frandsen, A. M., Mewaldt, R. A., et al. 1998, SSRv, 86, 1
26. Usoskin, I. G., Braun, I., Gladysheva, O. G., et al. 2008, JGR, 113, A07102 Usoskin, I. G., Kovaltsov, G. A., Adriani, O., et al. 2015, AdSpR, 55, 2940
27. Wawrzynczak, A., & Alania, M. V. 2010, AdSpR, 45, 622 Yermolaev, Y. I., Lodkina, I. G., Nikolaeva, N. S., & Yermolaev, M. Y. 2015,JGR, 120, 7094
28. Wawrzynczak, A., Ygbuhay, R., & Fikani, M.2014, SoPh, 289, 1763